

PARAMETRIC DESIGN & AN APPROACH TO WEIGHT OPTIMIZATION OF
A METALLIC AND CARBON FIBER WING

A Thesis

Submitted to the Faculty

of

Purdue University

by

John Joe

In Partial Fulfillment of the

Requirements for the Degree

of

Master of Science in Mechanical Engineering

August 2019

Purdue University

Indianapolis, Indiana

THE PURDUE UNIVERSITY GRADUATE SCHOOL
STATEMENT OF COMMITTEE APPROVAL

Dr. Hamid Dalir, Co-chair

Department of Mechanical and Energy Engineering

Dr. John F. Dannenhoffer III, Co-chair

Department of Mechanical and Aerospace Engineering

Dr. Carlos Larriba-Andaluz

Department of Mechanical and Energy Engineering

Approved by:

Dr. Jie Chen

Head of Graduate Program

This is dedicated to all people around the world who are taking risks.

Jumping in, in the name of engineering and innovation.

And to Ayrton Senna, who taught what it means to have a passion in life. And to
push for it, no matter the risk.

ACKNOWLEDGMENTS

I would like to express my sincere gratitude to my advisor Dr. Hamid Dalir and Dr. John F. Dannenhoffer III for their continued motivation, support, and guidance throughout my research work. I would also like to thank the member of the advisory committee, Dr. Carlos Larriba-Andaluz, for his insightful feedback and encouragement.

I express special appreciation to Mr. Christian Aparicio for his valuable inputs in MSC Nastran optimization and for sitting through all the skype meetings and the relentless questions and Mr. Julien Chaussee for his valuable inputs toward various types of analysis of different parts.

Additionally, I am grateful to all my colleagues at Advanced Composite Structures Engineering Laboratory (ACSEL), especially Souparna Satpati, Somesh Rath and Riddhi Joshi for their persistence in motivating me to write my thesis and graduate.

I would like to thank Mr. Jerry Mooney for his tireless efforts in reading this thesis, and helping me properly format my thesis.

This work was funded by the CAPS project, which was funded under AFRL Contract FA8050-14-C-2472: CAPS: Computational Aircraft Prototype Syntheses; Dr. Dean Bryson is the Technical Monitor. I would like to acknowledge the discussions with Dr. Nitin Bhagat, research engineer and AFRL contractor at the University of Dayton Research Institute during the formulation of various parts of these aircraft models.

I am thankful to IUPUI and the entire staff of the Department of Mechanical and Energy Engineering for financial assistance provided to me for this research work. I am also thankful to SCT Engineering College and Team Mec-Kartans where I took my first baby steps to where I am right now.

I would also like to thank Meghana Kamble who taught me I cannot treat people like an engineering or math problem and in general, shown me a different perspective to life and Viraj Gandhi for the stimulating technical conversations he had with me as well as doing everything ahead of the deadlines and leading the way and Rachana Solanki for your unlimited energy helping me overcome some of the most boring parts of my life.

Lastly, I would like to express my sincere gratitude towards my parents who supported me emotionally and financially during my graduate study and in my life in general, and especially my mom, who would regularly call me from across half the globe to ask me if I have turned in my submissions on time. Special thanks to my little brother for taking care of my parents while I was away from them.

TABLE OF CONTENTS

	Page
LIST OF TABLES	viii
LIST OF FIGURES	ix
ABBREVIATIONS	xi
ABSTRACT	xii
1 INTRODUCTION	1
2 PARAMETRIC DESIGN OF A COMMERCIAL AIRCRAFT USING EN- GINEERING SKETCHPAD	5
2.1 Commercial Aircraft Model Creation	5
3 AUTOMATED WEIGHT OPTIMIZATION OF ALUMINUM WING	12
3.1 Geometry Creation	12
3.2 Geometry Attribution	16
3.3 Results	18
4 OPTIMIZATION OF A COMPOSITE WING	21
4.1 Optimization Procedure	21
4.1.1 Step1	21
4.1.2 Step 2	21
4.1.3 Step3	22
4.2 CASE 1: FLAT PLATE	22
4.2.1 Geometry Creation and Meshing	22
4.2.2 Element Setup, Loads and Boundary Conditions	23
4.2.3 Results	23
4.3 CASE 2: WING	29
4.3.1 Geometry Creation and Meshing	29
4.3.2 Element Setup, Loads and Boundary Conditions	29

	Page
4.3.3 Results	32
5 CONCLUSION	44
REFERENCES	45

LIST OF TABLES

Table	Page
2.1 Design parameters for geometry creation of the commercial aircraft	9
2.2 Design parameters used to generate different internal structures	11
3.1 Design parameters used to create the wing and internals	16
4.1 Initial and Optimized Ply Orientations	24
4.2 Initial and Optimized Ply Thicknesses	29
4.3 Initial and Optimized Ply Thicknesses and Orientations	32
4.4 Initial and Optimized Ply Thicknesses and Orientations	43

LIST OF FIGURES

Figure	Page
2.1 The OML of the aircraft	6
2.2 The waffle structure used for creating the commercial aircraft.	6
2.3 The The union of the two waffles.	7
2.4 The internal structure with the stringers unioned.	7
2.5 The final aircraft model.	8
2.6 The ESP tree structure to generate a commercial aircraft.	8
2.7 Parametric generation of the OML and the internal structure of a commercial plane in ESP.	11
3.1 The wing OML creation.	12
3.2 The waffle for creating the internal structure.	13
3.3 The internal structure of the wing.	13
3.4 A panel with stiffeners generated.	13
3.5 The final wing model.	14
3.6 Geometric Attributes of the wing.	18
3.7 Attributes for the RBE3 nodes.	18
3.8 Attributes for each panel.	19
3.9 Optimized Aluminum Wing.	20
4.1 Model Setup.	23
4.2 Thickness distribution of Ply1.	24
4.3 Thickness distribution of Ply2.	25
4.4 Thickness distribution of Ply3.	25
4.5 Thickness distribution of Ply4.	25
4.6 Thickness distribution of Ply5.	26
4.7 Thickness distribution of Ply6.	26

Figure	Page
4.8 Thickness distribution of Ply7.	26
4.9 Thickness distribution of Ply8.	27
4.10 Model setup for Optimization.	28
4.11 Parametric Wing model created in ESP.	30
4.12 RBE3 load Application Area.	31
4.13 Thickness distribution of Ply1: Upper Skin.	33
4.14 Thickness distribution of Ply1: Lower Skin.	33
4.15 Thickness distribution of Ply2: Upper Skin.	34
4.16 Thickness distribution of Ply2: Lower Skin.	34
4.17 Thickness distribution of Ply3: Upper Skin.	35
4.18 Thickness distribution of Ply3: Lower Skin.	35
4.19 Thickness distribution of Ply4: Upper Skin.	36
4.20 Thickness distribution of Ply4: Lower Skin.	36
4.21 Thickness distribution of Ply5: Upper Skin.	37
4.22 Thickness distribution of Ply5: Lower Skin.	37
4.23 Thickness distribution of Ply6: Upper Skin.	38
4.24 Thickness distribution of Ply6: Lower Skin.	38
4.25 Thickness distribution of Ply7: Upper Skin.	39
4.26 Thickness distribution of Ply7: Lower Skin.	39
4.27 Thickness distribution of Ply8: Upper Skin.	40
4.28 Thickness distribution of Ply8: Lower Skin.	40
4.29 Wing model setup for Optimization: Upper Skin.	41
4.30 Wing model setup for Optimization: Lower Skin.	42

ABBREVIATIONS

attr	Attributes
CFD	Computational Fluid Dynamics
MPC	Multipoint Constraint
CSG	Constructive Solid Geometry
BRep	Boundary Representation
MDAO	Multidisciplinary Design, Analysis and Optimization
EGADS	Engineering Geometry Aircraft Design System
ESP	Engineering Sketch Pad
BEM	Built Up Element Model
OpenCSM	Open-source Constructive Solid Modeler
OML	Outer Mold Layer
IML	Inner Mold Layer
CAPS	Computational Aircraft Prototype Syntheses
UDP	User-Defined Primitive

ABSTRACT

Joe, John. M.S.M.E., Purdue University, August 2019. Parametric Design & an Approach to Weight Optimization of a Metallic and Carbon Fiber Wing. Major Professors: Dr. Hamid Dalir and Dr. John F. Dannenhoffer III.

In a multifidelity structural design process, depending on the required analysis, different levels of structural models are needed. Within the aerospace design, analysis and optimization community, there is an increasing demand for automatic generation of parametric feature tree (build recipe) attributed multidisciplinary models. Currently, this is mainly done by creating separate models for different disciplines such as mid-surface model for aeroelasticity, outer-mold line for aerodynamics and CFD, and built-up element model for structural analysis. Since all of these models are built independently, any changes in design parameters require updates on all the models which is inefficient, time-consuming and prone to deficiencies. In this research, Engineering Sketch Pad (ESP) is used to create attribution and maintain consistency between structural models with different fidelity levels. It provides the user with the ability to interact with a configuration by building and/or modifying the design parameters and feature tree that define the configuration. ESP is based on an open-source constructive solid modeler, named OpenCSM, which is built upon the OpenCASCADE geometry kernel and the EGADS geometry generation system. The use of OpenCSM as part of the AFRLs CAPS project on Computational Aircraft Prototype Syntheses for automatic commercial and fighter jet models is demonstrated. The rapid generation of parametric aircraft structural models proposed and developed in this work will benefit the aerospace industry with coming up with efficient, fast and robust multidisciplinary design standardization of aircraft structures. Metallic aircraft wings are usually not optimized to their fullest potential due to shortage of development time.

With roughly \$1000 worth of potential fuel savings per pound of weight reduction over the operational life of an aircraft, airlines are trying to minimize the weight of aircraft structures. A stiffness based strategy is used to map the nodal data of the lower-order fidelity structural models onto the higher-order ones. A simple multi-fidelity analysis process for a parametric wing is used to demonstrate the advantage of the approach. The loads on the wing are applied from a stick model as is done in the industry. C program is created to connect the parametric design software ESP, analysis software Nastran, load file and design configuration file in CSV format. This problem gets compounded when it comes to optimization of composite wings. In this study, a multi-level optimization strategy to optimize the weight of a composite transport aircraft wing is proposed. The part is assumed to initially have some arbitrary number of composite super plies. Super plies are a concept consisting of a set of plies all arranged in the same direction. The thickness and orientation angles of the super plies are optimized. Then, each ply undergoes topometry optimization to obtain the areas of each super ply taking the least load so that it could be cut and removed. Each of the super plies are then optimized for the thickness and orientation angles of the sub plies. The work presented on this paper is part of a project done for Air Force Research Laboratory (AFRL) connecting the parametric geometry modeler (ESP) with the finite element solver (Nastran).

1. INTRODUCTION

The overarching objective of this research is to develop a process to optimize any aircraft structure with a single click file execution. In the design, analysis and optimization of aerospace vehicles and structures, it is absolutely crucial to generate the geometry fast and in a robust way. For a given geometry, the number of structural solutions to support the design are unlimited. However, there is only one solution which could lead to the minimum weight for the structure. To realize this, a single common consistent parametric description of the design against different disciplines is necessary.

In Multi-Disciplinary Analysis and Optimization (MDAO) environments, it is a common practice to import the models from manufacturing design tools with usually IGES and STEP extensions. Although these structural parts and components are intended to be ultimately manufactured, the use of these extensions will create static (non-parametric) geometry models which are not intended for design optimization. Also, to create a Boundary Representation (BRep), the models should be closed watertight which is extremely difficult due to the lack of a complete solid modeling geometry kernel to deal with the topology data if any.

A web browser based integrated software referred to as the Engineering Sketch Pad (ESP) [1], is used here which completely resolves the issues mentioned above. ESP is built upon the WebViewer [2] and OpenCSM [3] and is fully parametric, attributed and is based on a feature-based solid-modeling system. OpenCSM in turn is built upon EGADS [4] and OpenCASCADE. All this software is open-source, freely available without licensing restrictions, and is in general use. [5]

The main objective here is to demonstrate through examples on how ESP could help the aerospace community by generation of parametric, feature-based analysis models to perform efficient MDAO. This would hopefully fill the existing gap between fully

realizable 3D representations and conceptual design and thus can be used to an advantage throughout the preliminary and detailed design stage.

Aircraft design at a conceptual level includes performing critical analysis on a low fidelity model and iterating different designs until the proposed design meets the design criteria. Out of the infinite possible solutions for the structural design, only one solution corresponds to the minimum weight. The process of culminating at this optimized structural design is an elaborate and computationally expensive process. The process is always a compromise between less complex models and faster iterations and more complex models and slower and expensive computations.

This process needs to be automated and is a major challenge in a design environment driven by optimization. The designer can not be expected to sift through the thousands of design cases to be analyzed for updating the geometry, the pre-processing or the post-processing. The goal here is to work towards a process that is completely automated.

The automatic generation of the geometry is only half of the solution. An interface that interlinks the geometry generation tool (ESP) and the analysis software is the ultimate goal. To attain this objective, a program is written in house using C.

The main objective of this research is to develop a methodology to automate the entire optimization process starting with the automatic generation of models, application of loads and boundary conditions, performing analysis, extracting the results data and comparing the results against failure to regeneration of the model with a safer or lighter design depending on the results and iterating till you achieve the minimum weight.

But, in today's world, a weight advantages that come from a well optimized metallic wing are just not going to be enough. In a world of ever-increasing demand of ultra-efficient and lightweight structures engineers and scientists are turning to composite materials. The industrial adoption of fiber reinforced composite materials entered a new era when several leading aircraft manufacturers started dropping a metal architecture and started designing and manufacturing essentially their air-

frame for commercial aircrafts using composite materials. Composite structures offer unprecedented design potential as the laminate material properties can be tailored almost continuously and variably throughout the entire structure by controlling each lamina individually.

There has been an accelerated deployment of structural optimization throughout all industries in the past decade, once they started noticing the tremendous efficiency gains that can be achieved at concept design stage through topology optimization [6] [7] [8] [9]. For conceptual design of structures, topology optimization has proven itself to be an extremely powerful tool that can generate new and innovative design concepts [10] [11] [12].

Composite materials are designed with an aim of achieving superior performance with unmatched thermomechanical properties and specific strengths, compared to even the best-case use of traditional materials. This increased design freedom, however, introduces new challenges for the design process and software.

Optimization of composite materials present a new set of challenges. The process of designing a lightweight component while maintaining robustness using composite materials component is a very complex, time consuming and generally difficult task. Not only do you have to account for many variables such as ply orientation, ply sequence, ply material, number of plies etc., but you must also take care to restrict some of these variables to discrete values.

It is also important to take a note of the industrial requirements and practical manufacturing constraints associated with composite materials. For example, an important design/manufacturing requirement mandated by FAA for aerospace structures is that when using unidirectional plies, no plies of identical orientation are allowed to be stacked continuously for more than 3 or 4 plies. Another example would be that composite laminate stackups are always tried to be made symmetric as well as balanced.

The design process of aerospace components consists of three phases. Conceptual design phase, initial design phase, and detailed design phase. The main objective of

this research is to develop a procedure for effective optimization [13] of composite structural members during the initial conceptual design phase of aerospace structures for a lightweight and robust structure.

2. PARAMETRIC DESIGN OF A COMMERCIAL AIRCRAFT USING ENGINEERING SKETCHPAD

This chapter shows the creation of a parametric model of a commercial aircraft. It discusses the basic procedure involving creation of the Outer Mold Line (OML) and waffle structures for the internals. The goal is to create an aircraft model which is entirely parametric, which needs not more than changing a few numbers to change all possible features of the model.

2.1 Commercial Aircraft Model Creation

Figure 2.1 through 2.5 shows different stages of the model generation process. Figure 2.1 depicts the Outer Mold Line (OML) of the aircraft which is the union of all the skins of the plane. Figure 2.2 is an extruded waffle to generate some of the internal aircraft structure which upon its intersection with the skin OML will result in the internal structure of the plane. The waffle for the vertical tail is intersected separately with the vertical tail and then is unioned with the main waffle. Figure 2.3 shows the union of the two horizontal and vertical waffles with only the two central stringers. The remaining stringers are intersected with the fuselage, rotated and then unioned with the waffle, thus forming the final internal structure of the aircraft as shown in Figure 2.4. The waffle structure is then subtracted from the OML to scribe it. This divides the OML into different skin panels intersected by the waffle. The scribed OML is then unioned with the internal structure and the Inner Mold Line (IML) is subtracted from the model. The resulting final model is shown in Figure 2.5.

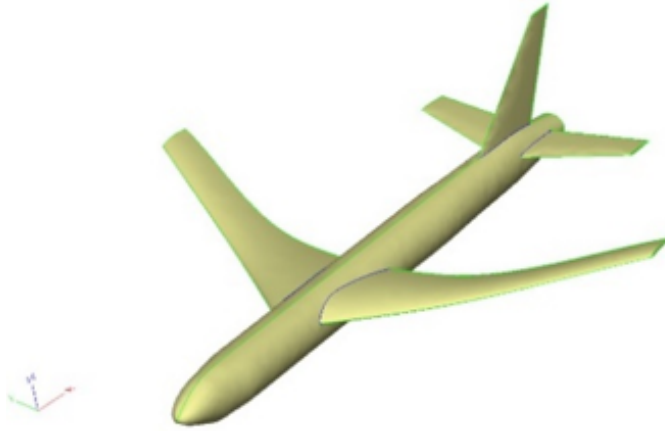


Fig. 2.1. The OML of the aircraft

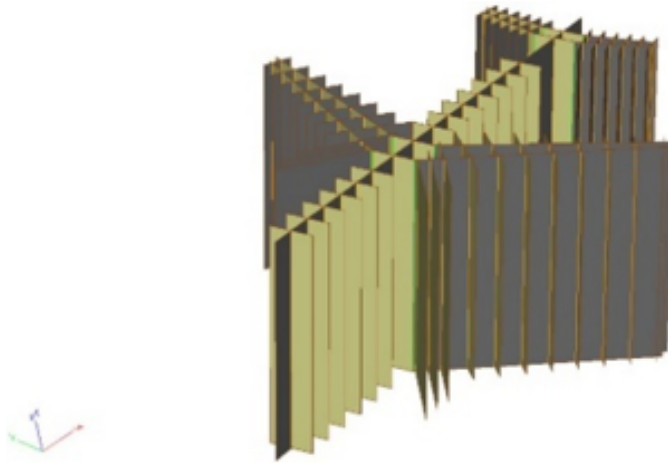


Fig. 2.2. The waffle structure used for creating the commercial aircraft.

The tree structure shown in Figure 2.6 explains the process involved in the generation of the commercial aircraft. The OML is generated by the union of the fuselage, the wing, the engine and the horizontal and vertical stabilizers, each of which are in turn generated using either the UDP blend for quadratic surface splines or UDP rule for linear surface splines from different profiles of the target solids. A parametric waffle is generated which contains the two central stringers as well as all the frames in the fuselage, the ribs and spars in the wing and the horizontal stabilizers. This waffle is intersected with the entire aircraft excluding the vertical stabilizer. A second waffle is

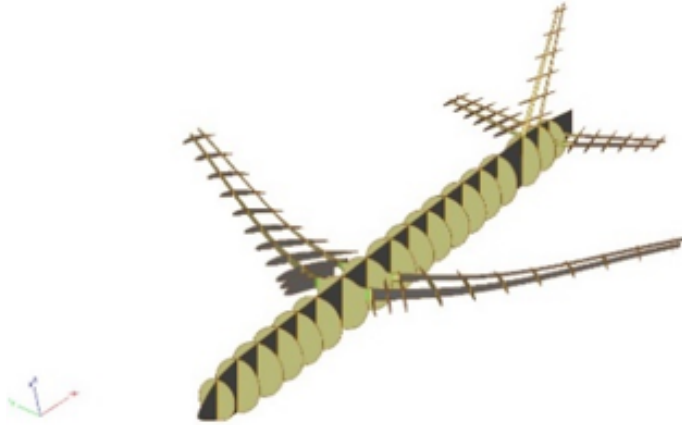


Fig. 2.3. The The union of the two waffles.



Fig. 2.4. The internal structure with the stringers unioned.

generated that corresponds to the internal structure of just the vertical stabilizer and the frames inside the vertical tail supporting it. The result model is intersected with the vertical stabilizer. The remaining protruding parts are removed by subtracting the horizontal stabilizers from this waffle. The two waffles are unioned together to form a single body. Sheet bodies are then created and rotated, forming the remaining stringers, and are then unioned to the join of the two waffles. The OML, which is a solid body is then extracted to generate a sheet body. The waffles are subtracted from the OML to scribe the OML with the internal structure. The internal structure

is then unioned with the OML to generate the final model. Table 2.1 shows the design parameters used in building the parametric model of the commercial aircraft.

Table 2.1.: Design parameters for geometry creation of the commercial aircraft

Parameter name	Value	Description
Fuse	[23x4] matrix	Dimensions of the fuselage(x,y,z1,z2)
noseList	[2x4] matrix	Curvature of nose cone in three directions
series_w	4409	NACA profile for the wing
wing	[3x5] matrix	x,y,z location, chord length & angle of attack of 3 profiles in wing
series_h	406	NACA profile for the horizontal stabilizer
xroot_h	14.5	Distance of root of horizontal stabilizer from nose
zroot_h	0.2	Distance of root of horizontal stabilizer from the central plane
aroot_h	0	Angle of attack of the horizontal tail at the tip
area_h	0.78	Area of the horizontal tail
taper_h	0.55	Taper ratio
aspect_h	3.7	Aspect ratio of the horizontal tail
sweep_h	25	Swept angle of the horizontal tail
dihed_h	3	Dihedral angle of the horizontal tail
twist_h	2	Twist angle of horizontal tail
series_v	404	NACA profile for the vertical stabilizer
xroot_v	13.2	Distance of root of horizontal stabilizer from nose

continued on next page

Table 2.1.: *continued*

Parameter name	Value	Description
zroot_v	0.4	Distance of root of horizontal stabilizer from central plane of plane
area_v	9.6	Area of the vertical tail
taper_v	0.3	Taper ratio of the horizontal tail
aspect_v	3	Aspect ratio of the vertical tail
sweep_v	45	Swept angle of the vertical tail
stringers_no	4	Number of stringers in one half plane (this ensures even number of stringers)
fore_frames_no	6	Number of frames between nose and wing
aft_frames_no	7	Number of frames between wing and vertical stabilizer
ribs_no	8	Number of ribs
iribs_no	3	Number of ribs in the region joining the wing and fuselage
hribs_no	6	Number of ribs in the horizontal stabilizer
vribs_no	6	Number of ribs in the vertical stabilizer
spars_no	2	Number of spars
vwing_ribs	4	Number of ribs in vertical wing

The three models shown in Figure 2.7 are different in terms of the configuration of their internal structures. The design parameters of each model have been depicted in Table 2.2. To create a new model with a new set of design parameters, one needs to vary the relevant design parameters. The new ESP model takes about 10 - 15 minutes to regenerate which will result in a fast and accurate multidisciplinary design optimization platform.



Fig. 2.7. Parametric generation of the OML and the internal structure of a commercial plane in ESP.

Table 2.2.

Design parameters used to generate different internal structures

	Number of ribs in the wing	Number of fore frames	Number of aft frames
Figure 2.3a	8	6	7
Figure 2.3b	5	3	4
Figure 2.3c	10	8	8

3. AUTOMATED WEIGHT OPTIMIZATION OF ALUMINUM WING

This chapter talks about how a parametric model of a wing is generated for automating optimization. The wing is optimized in Nastran for two of the most critical load cases. An API is used to optimize it against material failure and stability criterion. This chapter shows how ESP is extensively used to make process automated by making the geometry readable to the API.

3.1 Geometry Creation

To generate the wing and internal structure, (ESP) is used. ESP can generate geometry parametrically and create the built-up-element (BEM) ready for structural analysis. The input of ESP is written in a CSM file which is human readable and further can be edited using C program. CSM file is basically a script file which is read by ESP to generate geometry. Scripting capability enables minimum human

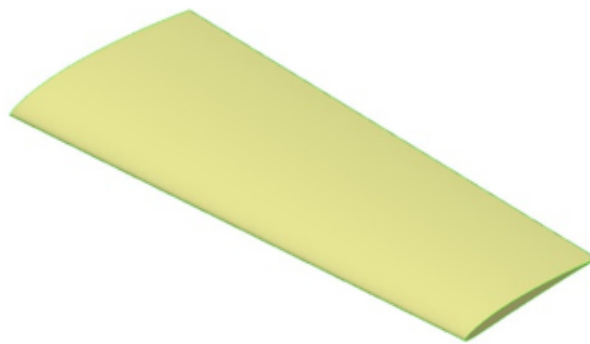


Fig. 3.1. The wing OML creation.

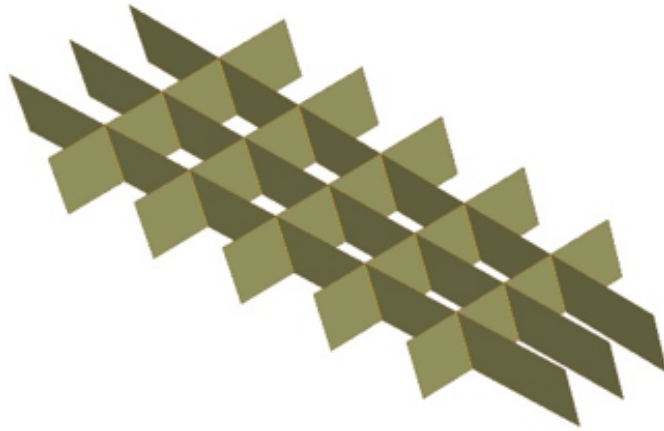


Fig. 3.2. The waffle for creating the internal structure.

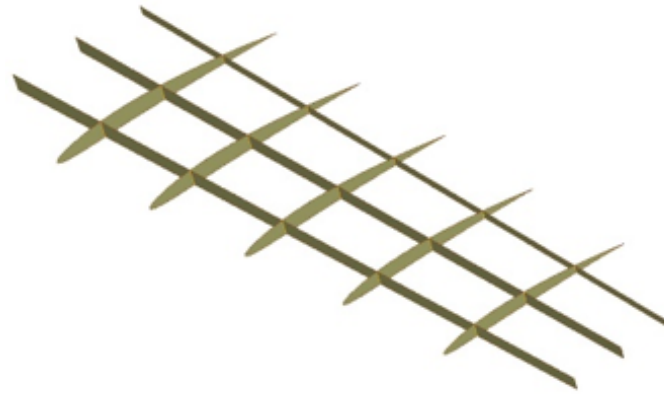


Fig. 3.3. The internal structure of the wing.



Fig. 3.4. A panel with stiffeners generated.

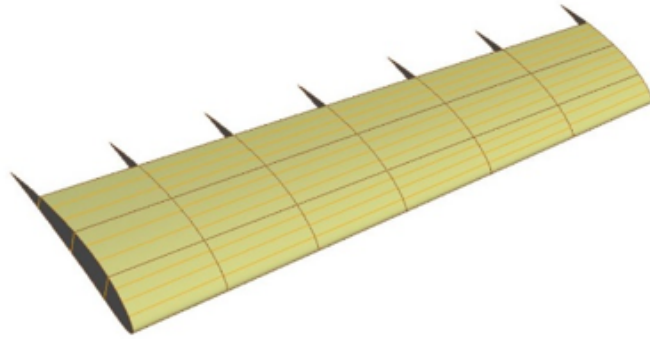


Fig. 3.5. The final wing model.

interaction which is another aim of this research. The mesh exported by ESP is mostly mapped mesh which is essential for buckling analysis.

ESP is based on geometry engine called OpenCSM. OpenCSM has unique capability to attribute each operation and geometry (i.e. Body, face, edge). In simpler words, feature of geometry and operations can be identified via name/value parameter which is useful in data transfer between different fidelity load transfer analyses. Also, attribute makes the multi-disciplinary transfer of loads and displacement between structures or models a nearly-trivial process. This feature is useful in the multi-disciplinary coupling analysis also.

Table 3.1 shows all the parameters that define the wing. The wing as shown in Figure 3.1 is modeled by creating two NACA profiles and connecting them by ruling them. The internals as shown in Figure 3.2 are created using the UDP 'waffle'. The UDP waffle allows the creation of a 2D sketch in the X-Y plane, which is then extruded in the Z direction. ESP allows the waffle to be created from a detailed text file which provides control over the geometry of the waffle. The details of the internals of the wing including the number of ribs and spars and the position of each component are input here. Figure 3.3 shows the waffle intersected with the OML of the wing generating the internal support structure.

More intricate details about the wing such as the stiffeners can be modelled using the UDP stiffeners. Stiffeners are critical in the conceptual design as they are responsible for the stability of the model under buckling. UDP stiffener enables generating runoffs at both ends of the stiffeners.

Further, to optimize wing for local buckling analysis, each panel needs to be stiffened. The stiffeners do not play an important role for material failure, but they are very important for stability. For that, the panels are imported one by one and stiffened using UDP stiffeners. UDP stiffeners creates surface perpendicular to the local surface on panel for given depth. It also generates runoffs at the end of stiffeners. Figure 3.4 shows the panel with stiffeners. Figure 3.5 demonstrates the entire wing with all individual panels stiffened.

Table 3.1.
Design parameters used to create the wing and internals

Parameter name	Value	Description
series_w	4409	NACA profile of the wing
area	10	area of the wing
aspect	6	aspect ratio of the wing
taper	0.7	taper ratio of the wing
sweep	20	sweep angle of the wing
nrib	5	number of ribs in the wing
xfirst	0.2	fraction distance in the chordwise length of the first spar
xlast	0.75	fraction distance in the chordwise length of the last spar
nspar	3	number of spars in the wing
nstiff	3	number of stiffeners on the wing panel
depth	-0.01	depth of the stiffener
angle	45	angle of the runoffs at the ends of the stiffener

3.2 Geometry Attribution

Attributes on geometries are consistent upon further operations. For example, if upper wing surface is attributed as upper surface, and if that surface is divided into several panels, each panel will have same attribute upper surface. Another example is intersection in waffle. The whole surface will retain the attribute tagType=Rib and tagIndex=1 as shown in Figure 3.6. Also, a geometry can have any number of attributes can be given as long as the name of the attribute is different in name/value combination. That is particularly useful in case of differentiating wing panels. Panels are identified by pair of neighboring ID of ribs and spar; the upper panel and lower panel can be identified easily. For example, two panels may have the same attribute

U3.4. But they can be differentiated by another attribute, Upper Surface/Lower Surface. ESP maintains attributes on the geometries if dumped in its own format that is, EGADS.

In the following section, detailed method of wing creation and attribution is displayed which is used in further analysis. Firstly, two naca profiles are created based of parameters provided by user (given in table) then they are ruled to create Outer Mold Layer (OML) of wing. The upper surface is attributed as `upper_skin` and lower surface as `lower_skin`. The leading edge and trailing edge are attributed as `leading_edge` and `trailing_edge`. The waffle is created based on user parameters. The waffle is subtracted from wing to create panels. Which is called as scribed wing. To make internal structure, waffle is intersected with non-scribed wing so that the ribs will have shape of naca profile automatically and height of spar will also set automatically. The scribed wing is converted to sheet body by `extract` command. And for the last step, internal structure is united with scribed-sheet-wing. While making waffle, each ribs and spars are given attributes. Ribs are identified as `name = Rib` and `index = 1,2,3, etc.` The root rib is given `index = 0` and tip rib is given `index = nRib+1`. The spars are identified as `name = Spar` and `index = 1,2,3, etc.` Based on attributes on face of ribs and face of wing, edge attribute called `RBE3_1,2,3, etc.` is given as shown in Figure 3.7. These attributes are important to create RBE3 elements. Based on these attributes, each panel is attributed in the loop. The example of attributions is given in figures. The surfaces attached to trailing edge is given attribute as `ignoreNode=true` which allows the element associated with the surfaces to not to come in. `bdf` file. The `bdf` file is then generated using `createBEM` UDF. Each panel is dumped with extension of, EGADS so that the panels will retain their attributes upon importing it to ESP again. This `bdf` file is used to perform static structural analysis on wing.

The edges of unstiffened panels are attributed as `outside` as shown in Figure 3.8. This will be later useful for data transfer from global wing analysis to local panel analysis. All the CSM scripts are edited by C code and being executed by ESP automatically.

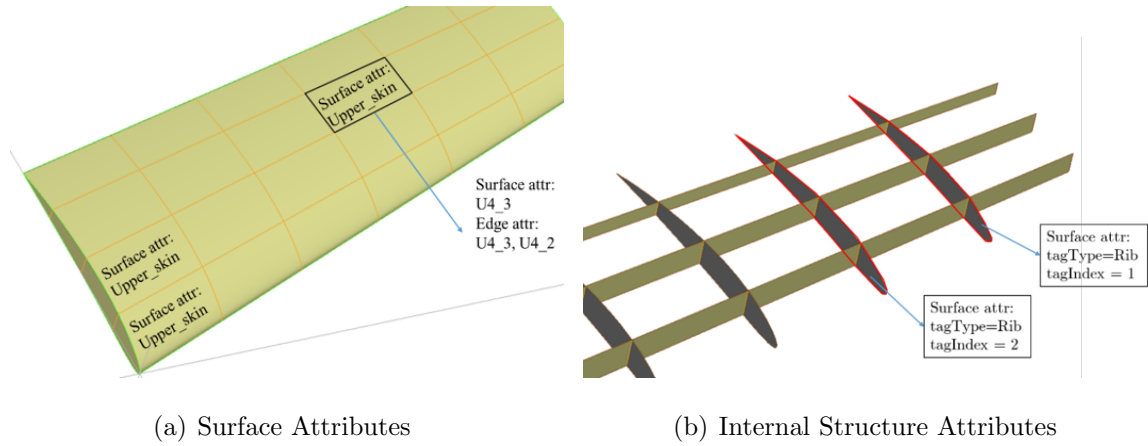


Fig. 3.6. Geometric Attributes of the wing.

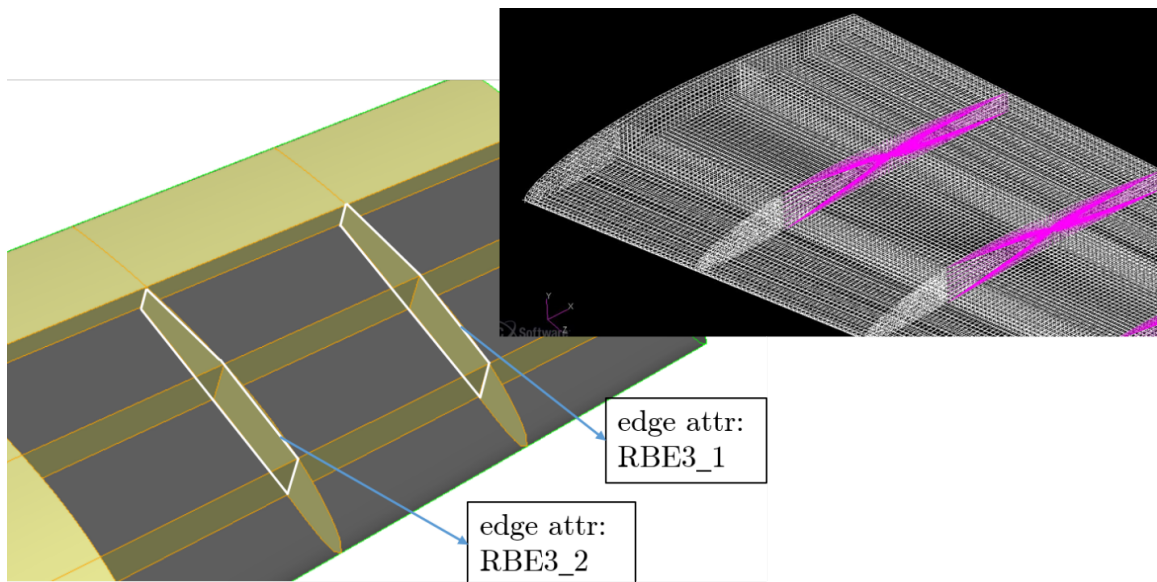


Fig. 3.7. Attributes for the RBE3 nodes.

3.3 Results

The API performs the optimization on the wing for material failure and on each stiffener for stability and outputs the number of ribs, the number of stiffeners in each panel and the thicknesses of the ribs, spars, stiffeners and the skin. The range of

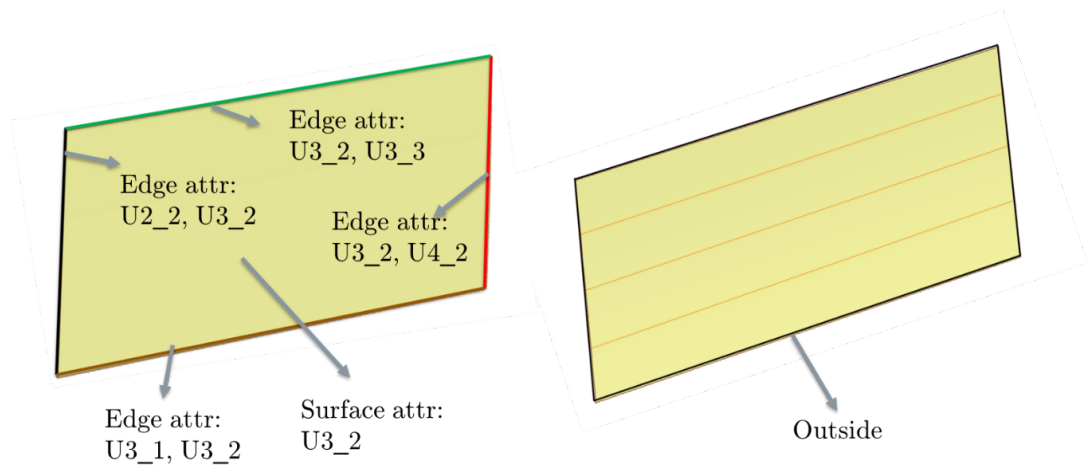


Fig. 3.8. Attributes for each panel.

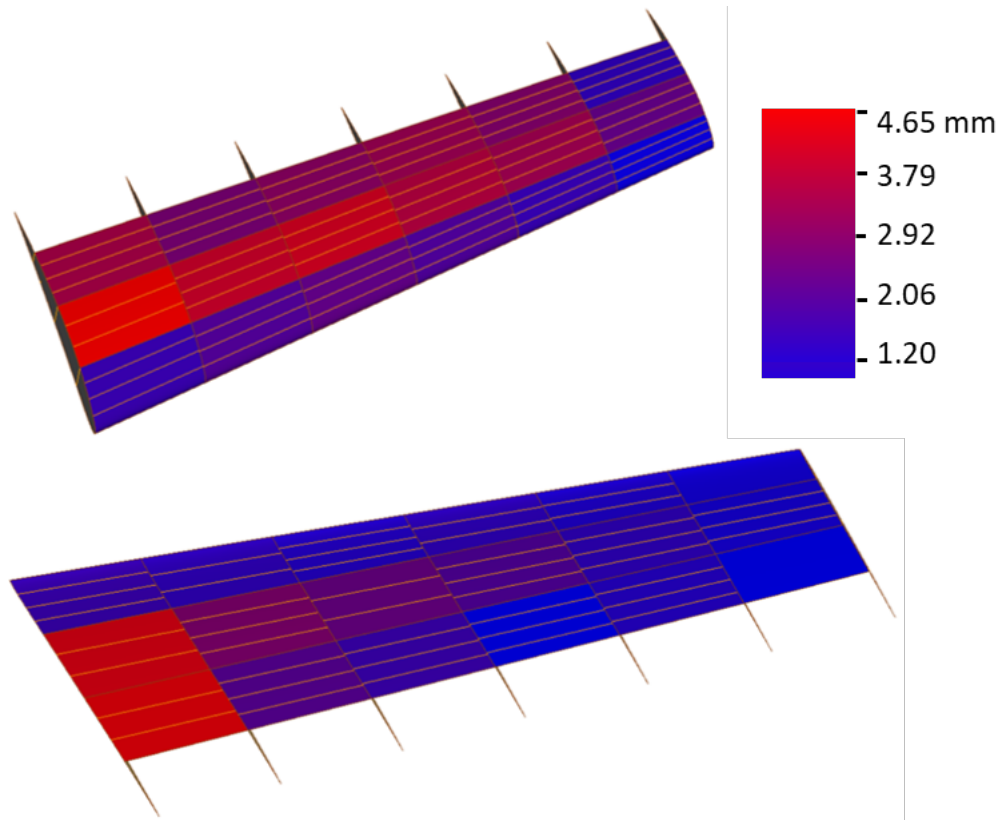


Fig. 3.9. Optimized Aluminum Wing.

thicknesses for all surfaces is 8mm to 1mm. Number of ribs varies from 3 to 6 and number of spars are fixed 3. Number of stiffeners varies from 0 to 4. The results of overall optimized geometry has 5 ribs and 3 spars. The rib thickness is 1.19mm and spar thickness is 4.47 mm. the overall weight of the wing is 84.6 kg. The optimized wing is shown in Figure 3.9.

4. OPTIMIZATION OF A COMPOSITE WING

This chapter talks about optimization of a composite wing. The same geometry is used for the composite wing that was used for the aluminum wing. An attempt has been made to develop a methodology for optimizing a composite wing.

4.1 Optimization Procedure

The optimization procedure involves 3 steps.

4.1.1 Step1

We start by assuming an arbitrary number of plies in the model. These plies are thicker than they practically can be to have a reasonable starting point. These unreasonably thick plies will hence be called super plies. A size optimization is performed for maximum stiffness using MSC NASTRAN with the orientations and the thicknesses of the super plies as the optimization variables. A size optimization keeps the element properties constant throughout the element. This ensures that each finite element has the same thickness and orientation as the adjacent elements. This is to ensure ply continuity in terms of thickness and orientation all over the model. The target of this phase is to obtain the material distribution in terms of thickness and orientation. This step outputs the optimum thickness and orientations angles of the super plies.

4.1.2 Step 2

The next step is a topology optimization. In this step each finite element is considered as an independent design variable. The solver applies the load and finds the

elements that carry the least loads (the least critical elements) keeping the thickness and the orientation from step 1. The idea behind this step is identify the areas of the model which can be removed from each ply. The optimizer outputs the low thickness areas of each ply which are then removed. This process is not so straight forward as there is only element representing all the plies at one location. To obtain the ply cutoffs, the elements are divided into different areas depending on the element thickness distribution and each area is given their respective laminate stackup sequence. To summarize, at the end of this step, the orientations of the super plies and the ply cutoffs are known.

4.1.3 Step3

This is again, a size optimization. But, this time only the ply thicknesses are optimized with the ply cutoffs applied and the orientation angles fixed. Once the thicknesses of the super plies are obtained, we can divide the thickness of the super ply with the thickness of the actual carbon fiber ply to get the number of plies required in that region.

The optimization was done first on a simple square plate to understand and to figure out the kinks of the procedure and was then done on the wing.

4.2 CASE 1: FLAT PLATE

4.2.1 Geometry Creation and Meshing

The geometry used was a simple rectangular flat plate consisting of only 2D shell elements. The model was meshed with exclusively CQUAD4 elements. The geometry was created and meshed in PATRAN.

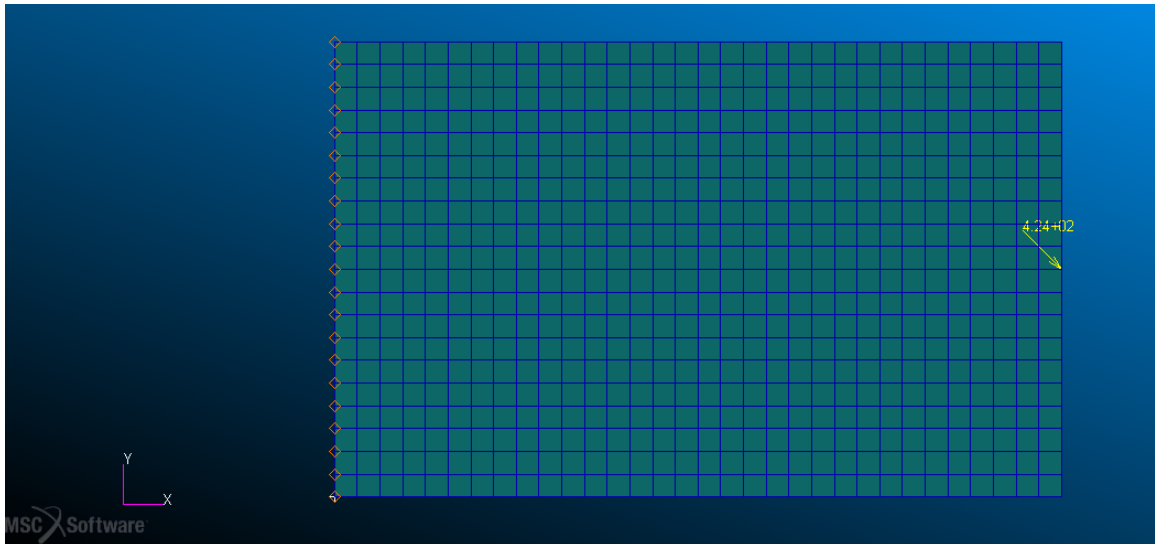


Fig. 4.1. Model Setup.

4.2.2 Element Setup, Loads and Boundary Conditions

The model is assumed to have a total of 16 plies, with an 8 ply symmetric stackup. All elements are of the property type PCOMP used to represent carbon fiber. The left edge of the plate is constrained in all six degrees of freedom. A load of 300N is applied in the positive X as well as the negative Y direction on the central node of the right edge. Figure 4.1 shows the model setup.

4.2.3 Results

Step 1: Size Optimization

Due to the simplicity of the model, only the ply orientations are optimized in this step. The ply thicknesses are not optimized. Table 4.1 shows the initial and the optimized orientations. Since the laminate stackup is symmetric, only one half of the symmetry is discussed here. The initial orientation angles -65° and 80° were chosen arbitrarily.

Table 4.1.
Initial and Optimized Ply Orientations

Ply Orientation Angles	Initial values	Optimized values
Ply1	80°	61°
Ply2	-65°	-60°
Ply3	80°	61°
Ply4	-65°	-60°
Ply5	80°	61°
Ply6	-65°	-60°
Ply7	80°	61°
Ply8	-65°	-60°

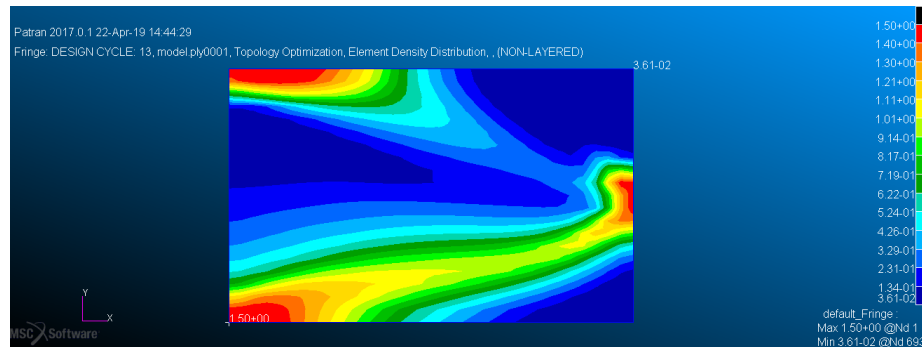


Fig. 4.2. Thickness distribution of Ply1.

Step 2: Topometry Optimization

These images show the thickness distribution for the 8 plies. The blue area represents areas that carry minimal loads and the red areas carry the maximum loads. Figures 4.2 - 4.9 show the thickness distribution of the plies after topometry optimization. The thickness distributions for alternating plies are identical as they share the same orientation angle.

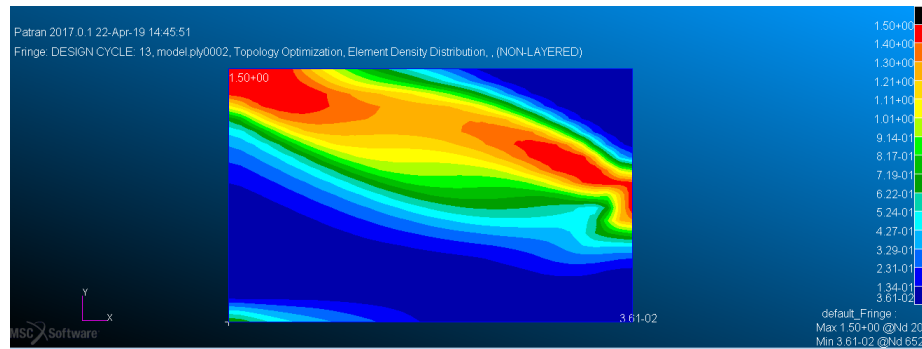


Fig. 4.3. Thickness distribution of Ply2.

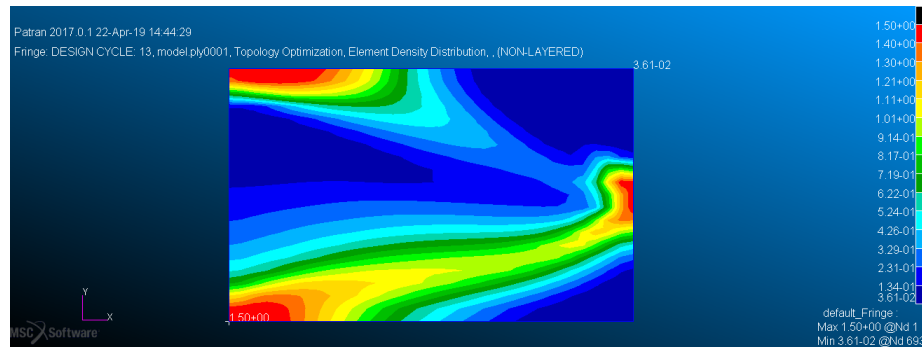


Fig. 4.4. Thickness distribution of Ply3.

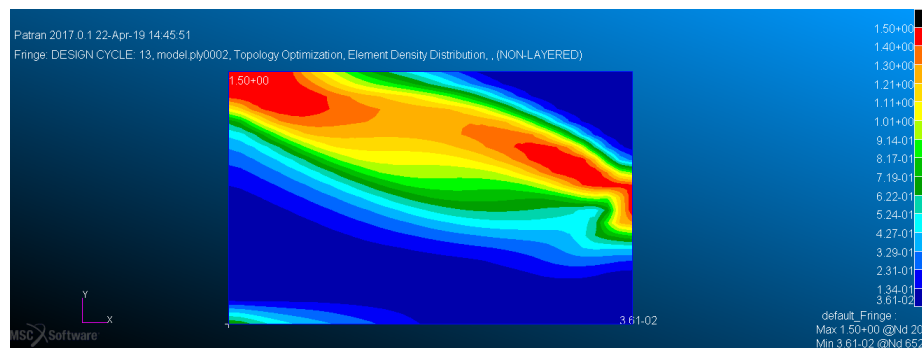


Fig. 4.5. Thickness distribution of Ply4.

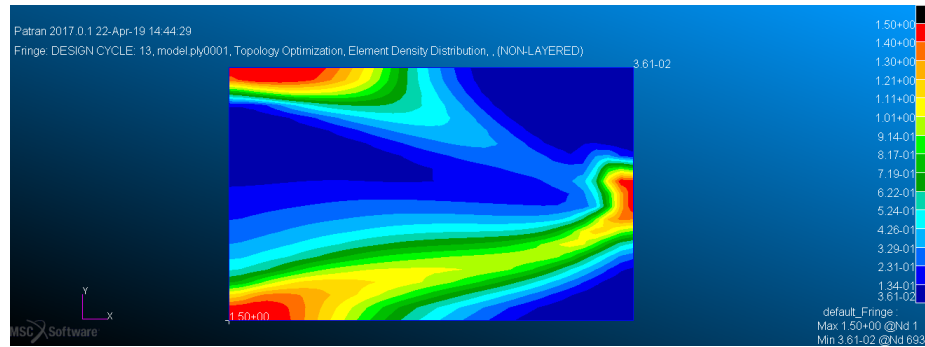


Fig. 4.6. Thickness distribution of Ply5.

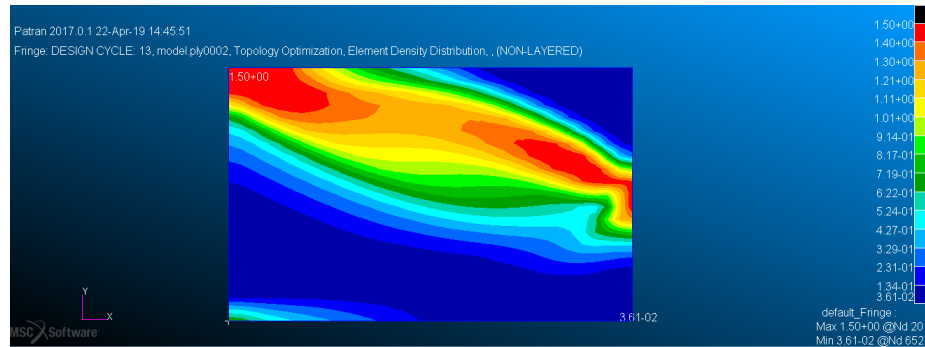


Fig. 4.7. Thickness distribution of Ply6.

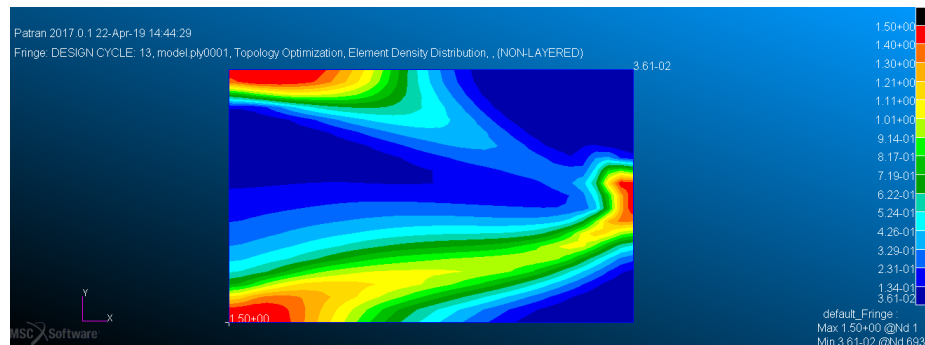


Fig. 4.8. Thickness distribution of Ply7.

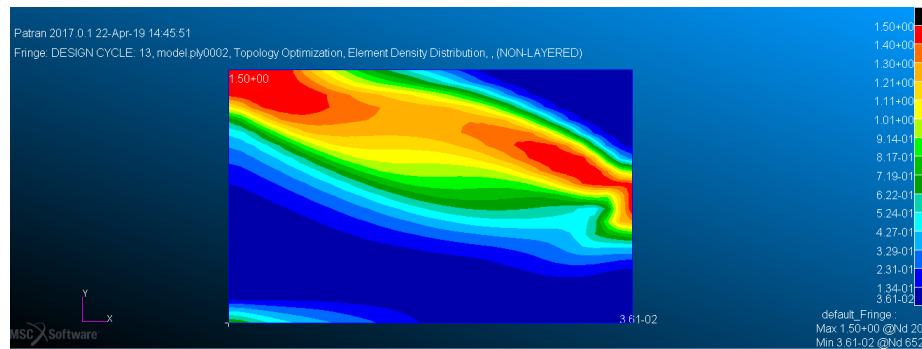


Fig. 4.9. Thickness distribution of Ply8.

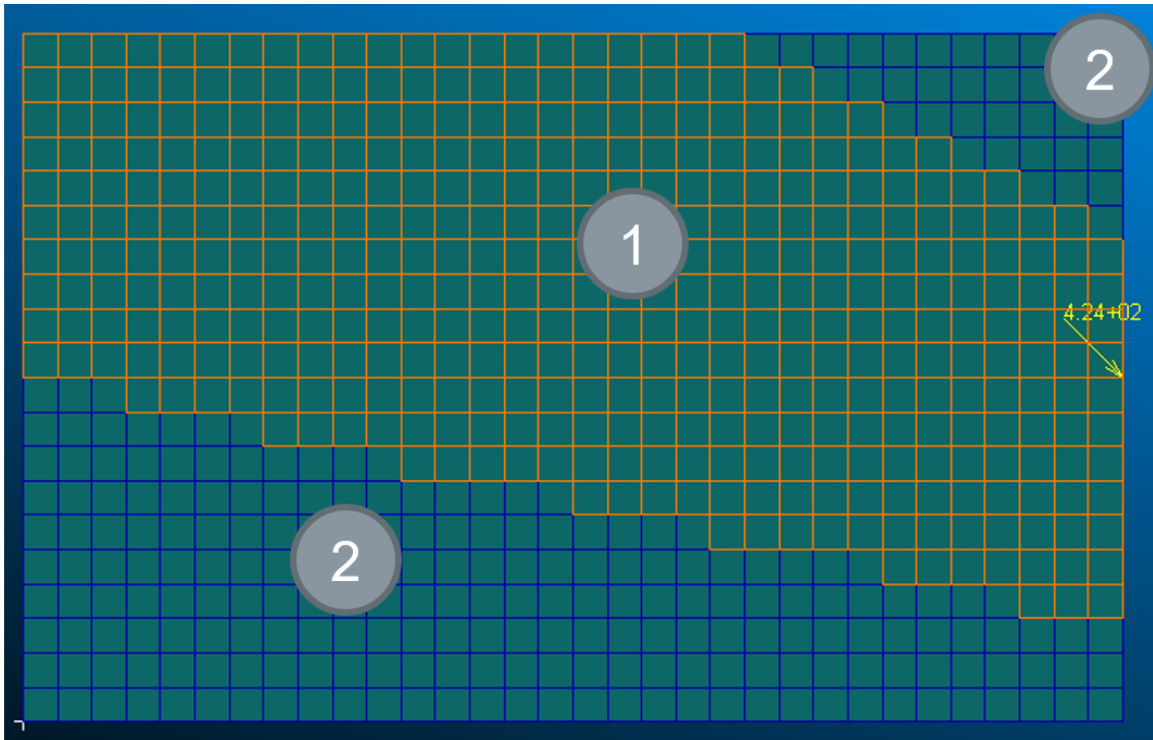


Fig. 4.10. Model setup for Optimization.

Step 3: Size Optimization

The ply thicknesses are optimized for the applied load keeping the ply orientations constant. The model is divided into 2 areas according to the results from the topology optimization. Area 1 has a stackup of $[61^\circ/-60^\circ/61^\circ/-60^\circ/61^\circ/-60^\circ/61^\circ/-60^\circ]$ s. Area 2 has a stackup of $[61^\circ/61^\circ/61^\circ/61^\circ]$ s. Figure 4.10 shows the model setup for the optimization. Table 4.2 shows the final values for the ply orientation and thicknesses.

Table 4.2.
Initial and Optimized Ply Thicknesses

Ply Thicknesses	Initial Value	Optimized value
Ply1	1 in	0.001 in
Ply2	1 in	0.00246 in
Ply3	1 in	0.001 in
Ply4	1 in	0.00246 in
Ply5	1 in	0.001 in
Ply6	1 in	0.00246 in
Ply7	1 in	0.001 in
Ply8	1 in	0.00246 in

4.3 CASE 2: WING

4.3.1 Geometry Creation and Meshing

ESP was used for the generation of the wing. The wing was created as a parametric model with the geometry and the internals to be regenerated to any desired shape, size or number by changing a few numbers. This helps in rapid regeneration of different geometries to do analysis on. The wing model consists entirely of 2D shell elements. The meshing was done in ESP. the model used in this optimization has two spars and five ribs. Figure 4.11 shows the wing in ESP.

4.3.2 Element Setup, Loads and Boundary Conditions

The model is assumed to have a total of 16 plies, with an 8 ply symmetric stackup. The elements in the skin of the wing are of the property type PCOMP representing carbon fiber. The elements in the ribs and spar are aluminum and have the property type PSHELL. The face of the root of the wing contained by the wing box is

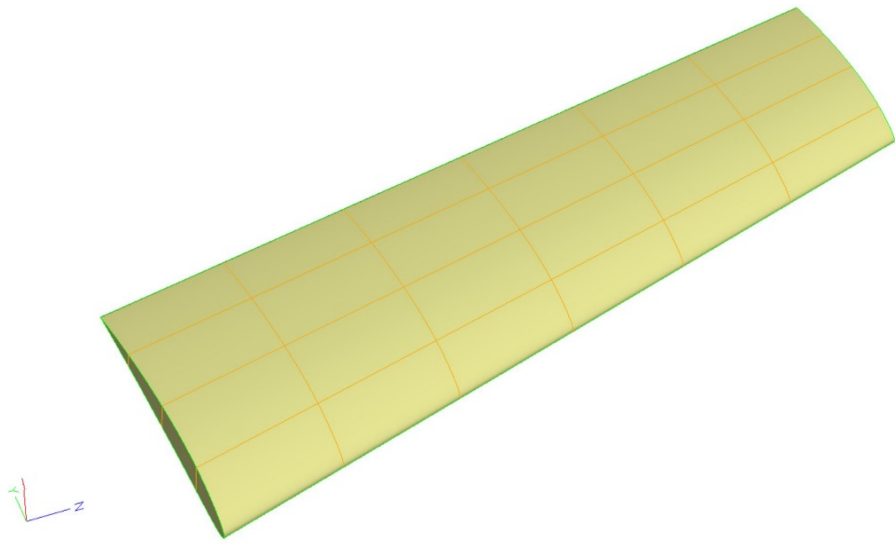


Fig. 4.11. Parametric Wing model created in ESP.

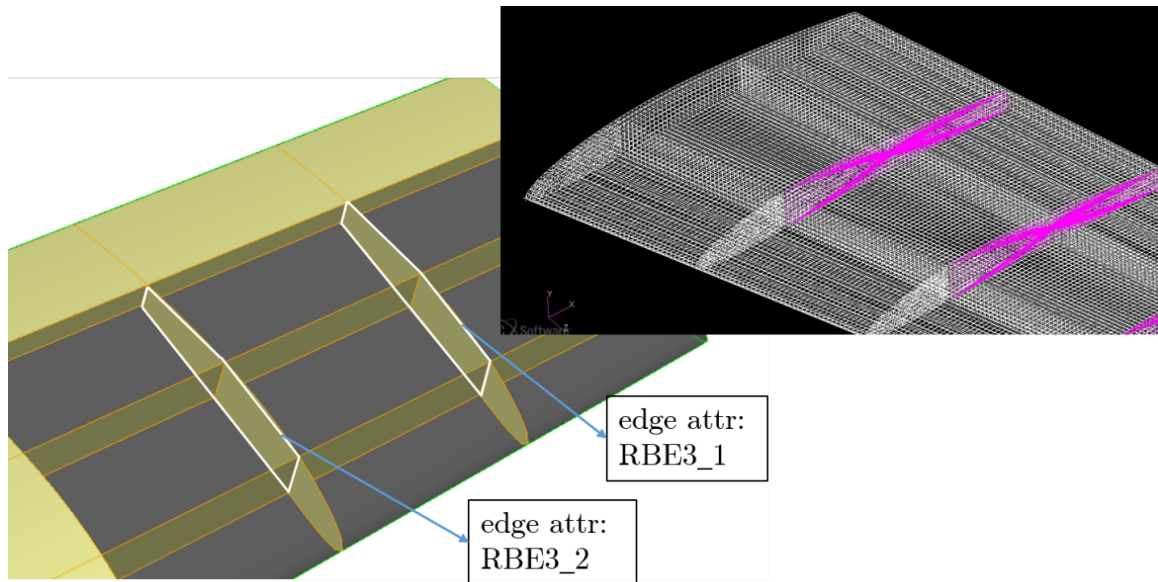


Fig. 4.12. RBE3 load Application Area.

constrained in all six degrees of freedom. The loads are simulating an extreme aerodynamic load case of a 2.5g upbend, which is experienced on the wing at liftoff. The loads from the CFD analysis are transferred to the structural model for analysis using a stick model. The stick model condenses the aerodynamic pressures into forces and moments onto a few nodes that can be transferred easily. The stick model approach for loading was used as it is the approach used in the aviation industry. The loads from the stick model are applied on the wing using RBE3 nodes. RBE3 nodes are used to distribute loads from a single point to an area or an edge. The load is transferred from the master node to the slave nodes as an inverse proportion to the distance between the master and slave nodes. The RBE3 master nodes are located on the rib of the wing at the center of the face enclosed within the wing box. The RBE3 slave nodes are the boundary nodes of the ribs inside the wing box. Figure 4.12 shows the master and slave RBE3 nodes and the area in which it is applied.

4.3.3 Results

Step 1: Size Optimization

Due to of the complex geometry and the intricacies of the model, both the ply orientations and ply thicknesses are optimized in this step. Table 4.3 shows the initial and the optimized thicknesses and orientations.

Table 4.3.
Initial and Optimized Ply Thicknesses and Orientations

Thicknesses and Ply Orientations	Initial values		Optimized values	
	Orientation	Thickness	Orientation	Thickness
Ply1	-45°	0.250 mm	-45°	0.511 mm
Ply2	45°	0.250 mm	90°	0.512 mm
Ply3	-45°	0.250 mm	-45°	0.503 mm
Ply4	45°	0.250 mm	0°	0.492 mm
Ply5	-45°	0.250 mm	0°	0.500 mm
Ply6	45°	0.250 mm	45°	0.491 mm
Ply7	-45°	0.250 mm	0°	0.501 mm
Ply8	45°	0.250 mm	0°	0.491 mm

Step 2: Topometry Optimization

Figures 4.13 4.28 show the thickness distribution for the upper and lower skin respectively for the 8 plies. The blue area represents areas that carry minimal loads and the red areas carry the maximum loads.

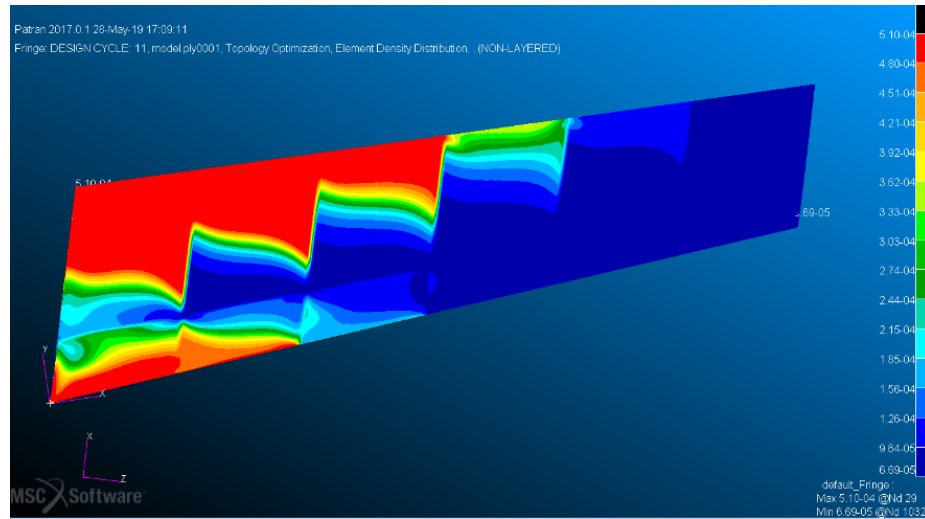


Fig. 4.13. Thickness distribution of Ply1: Upper Skin.

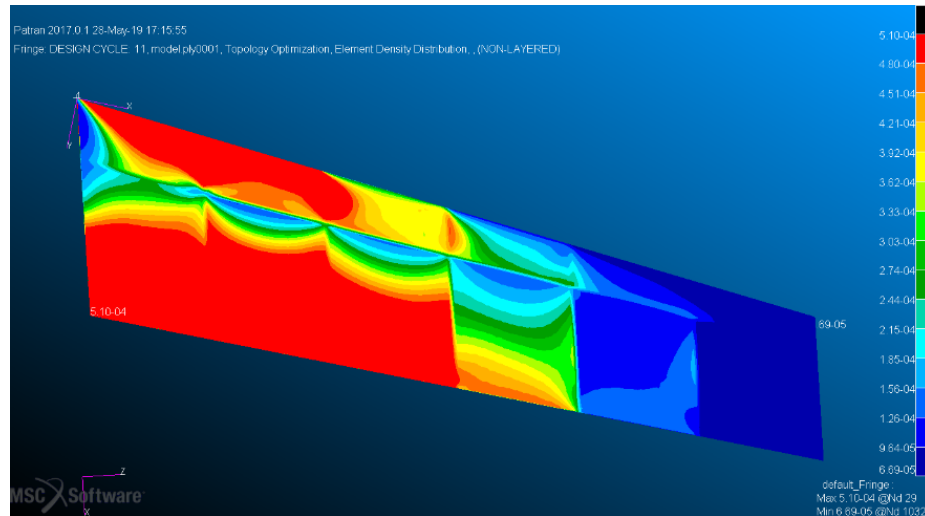


Fig. 4.14. Thickness distribution of Ply1: Lower Skin.

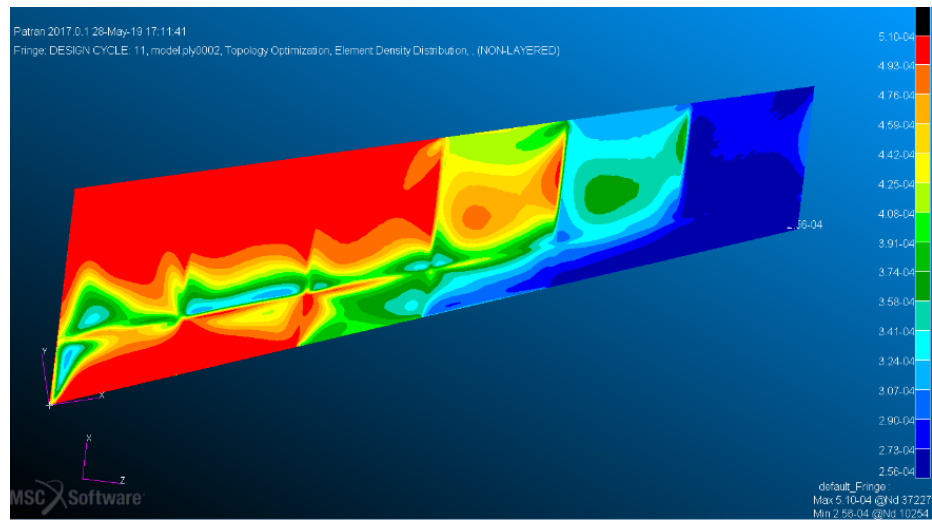


Fig. 4.15. Thickness distribution of Ply2: Upper Skin.

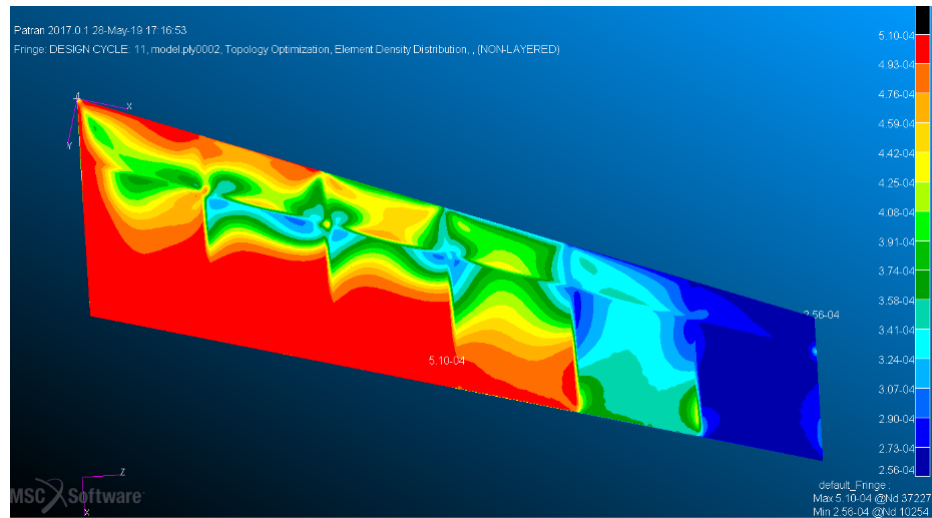


Fig. 4.16. Thickness distribution of Ply2: Lower Skin.

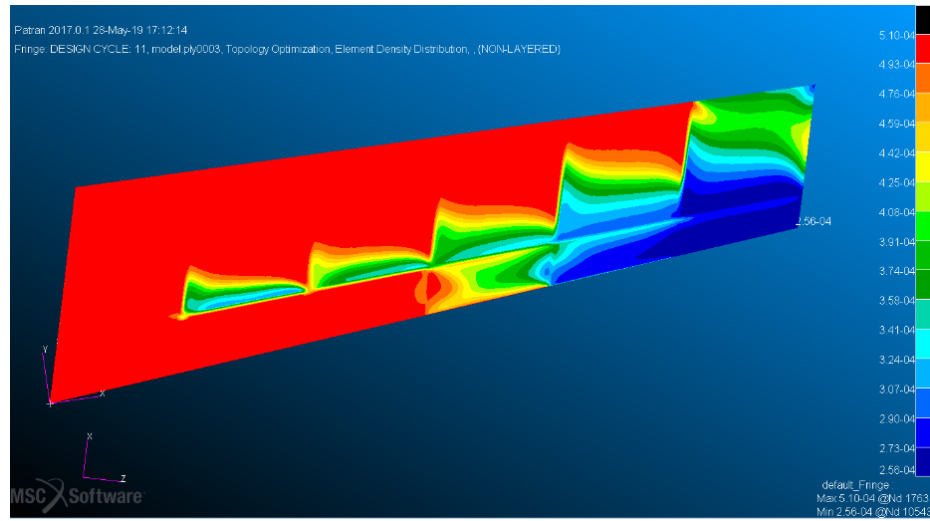


Fig. 4.17. Thickness distribution of Ply3: Upper Skin.

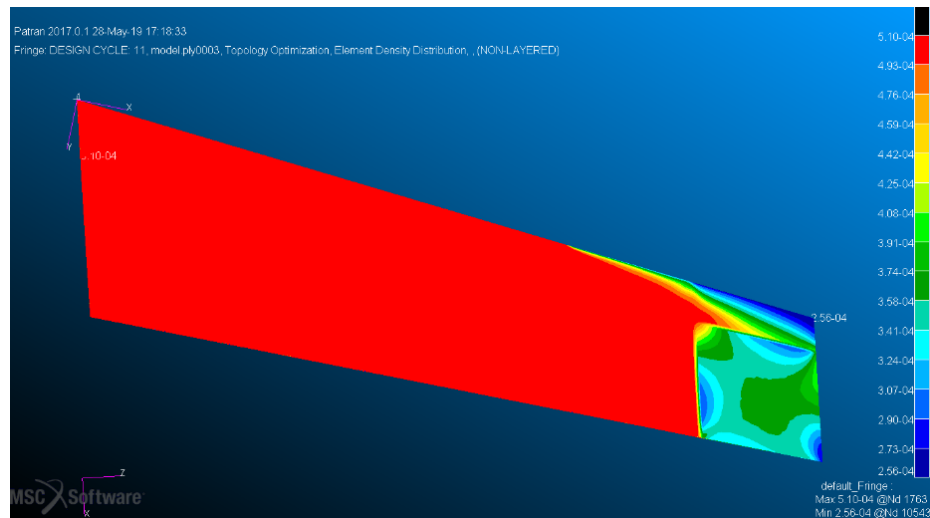


Fig. 4.18. Thickness distribution of Ply3: Lower Skin.

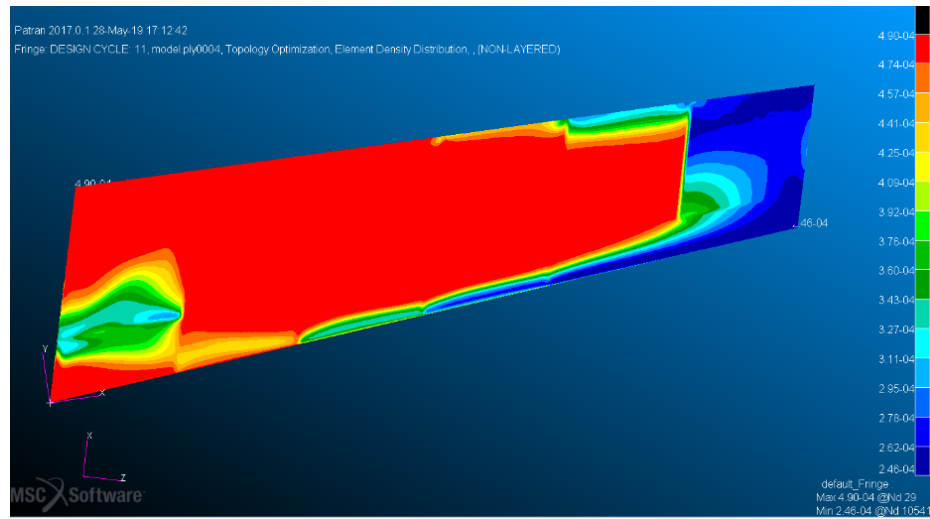


Fig. 4.19. Thickness distribution of Ply4: Upper Skin.

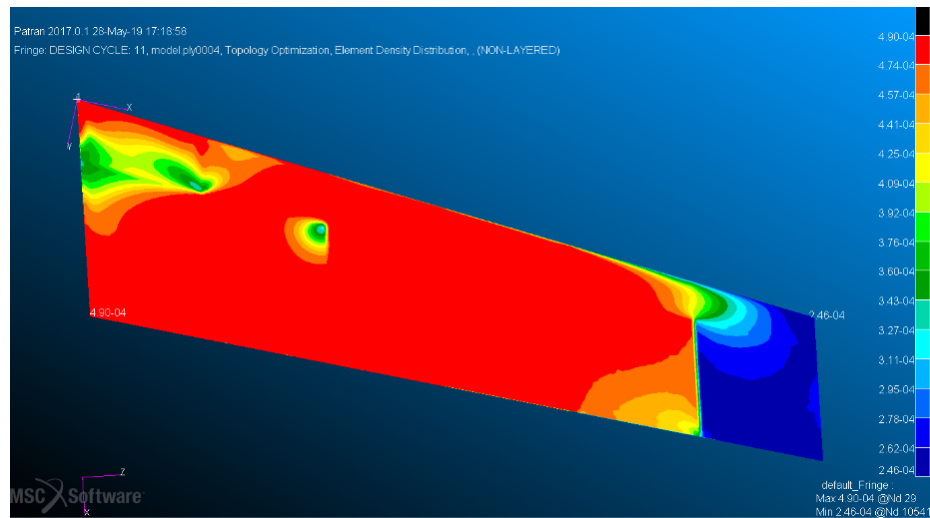


Fig. 4.20. Thickness distribution of Ply4: Lower Skin.

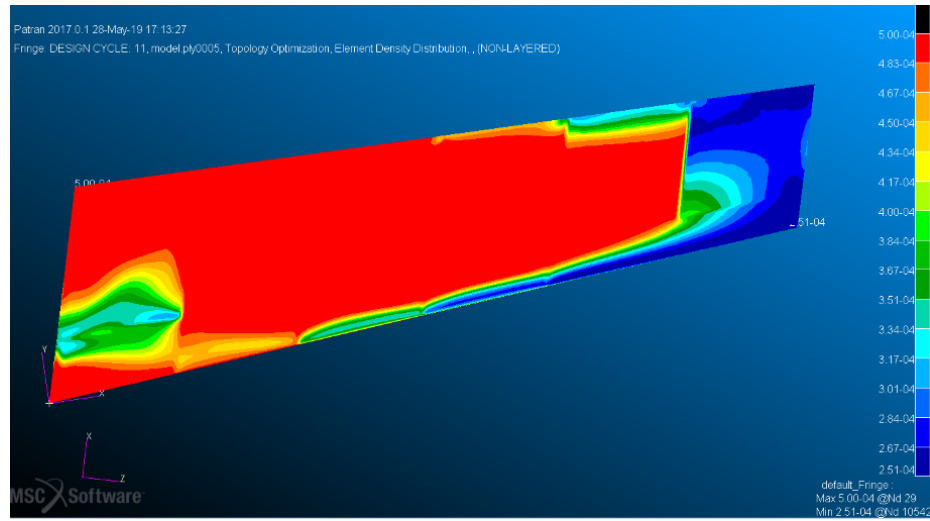


Fig. 4.21. Thickness distribution of Ply5: Upper Skin.

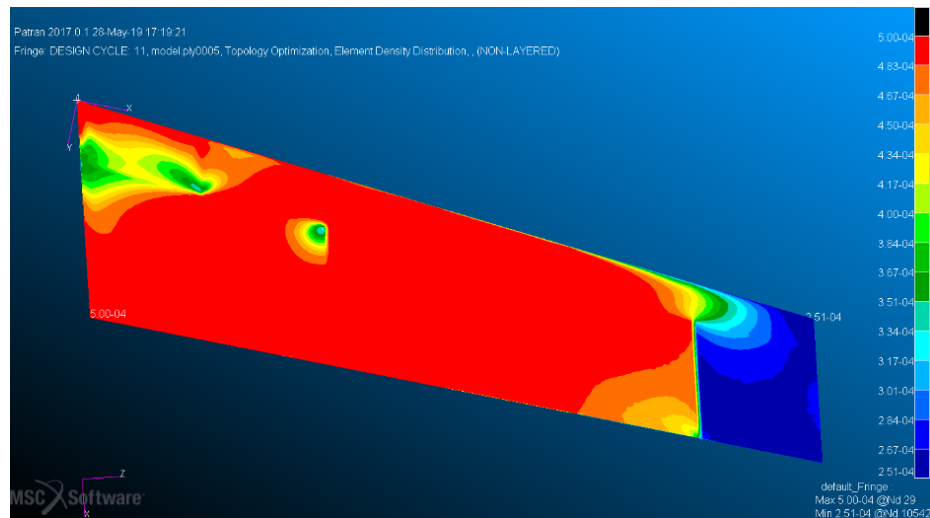


Fig. 4.22. Thickness distribution of Ply5: Lower Skin.

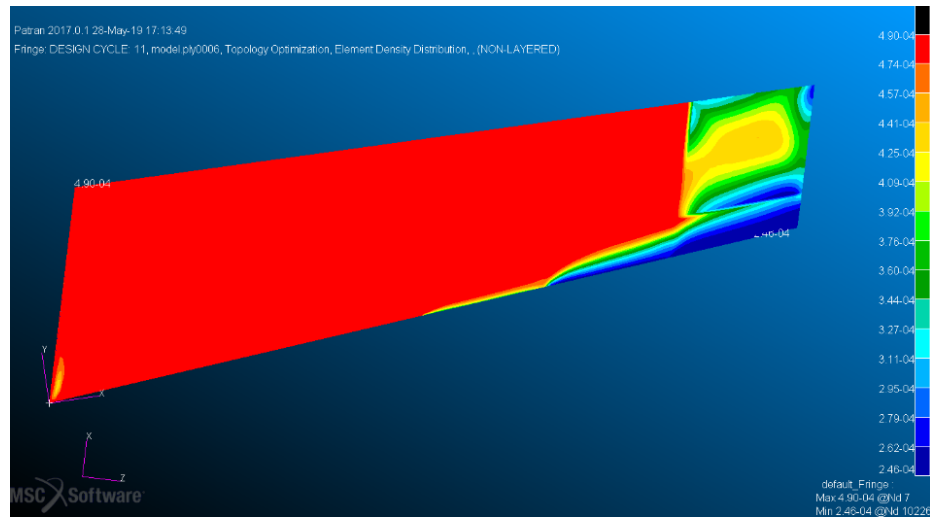


Fig. 4.23. Thickness distribution of Ply6: Upper Skin.

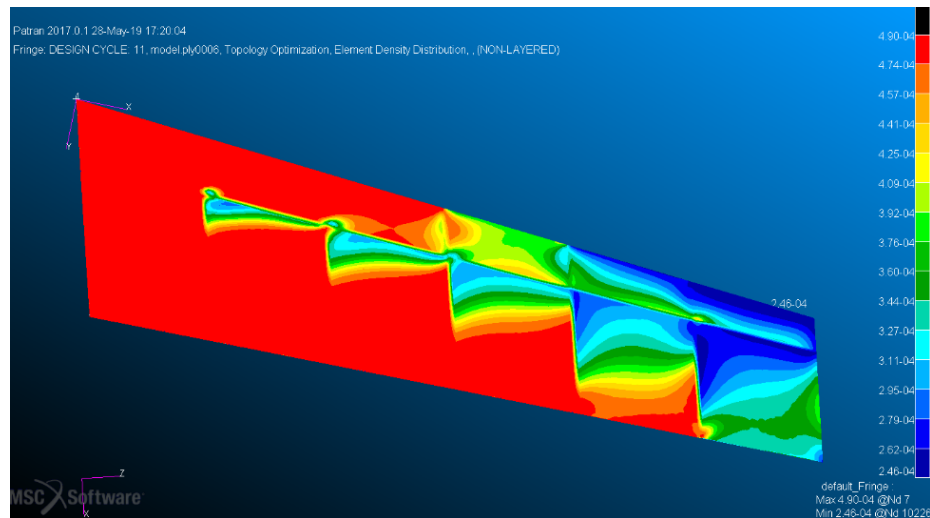


Fig. 4.24. Thickness distribution of Ply6: Lower Skin.

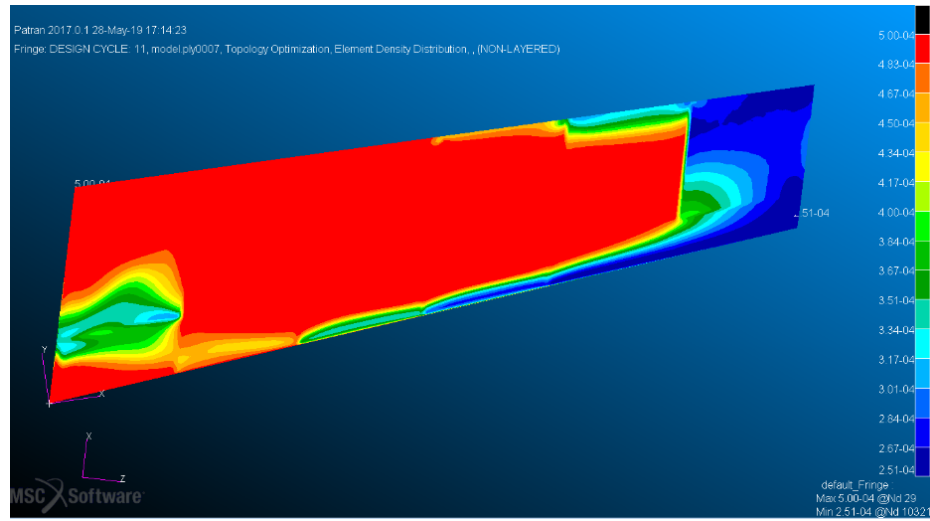


Fig. 4.25. Thickness distribution of Ply7: Upper Skin.

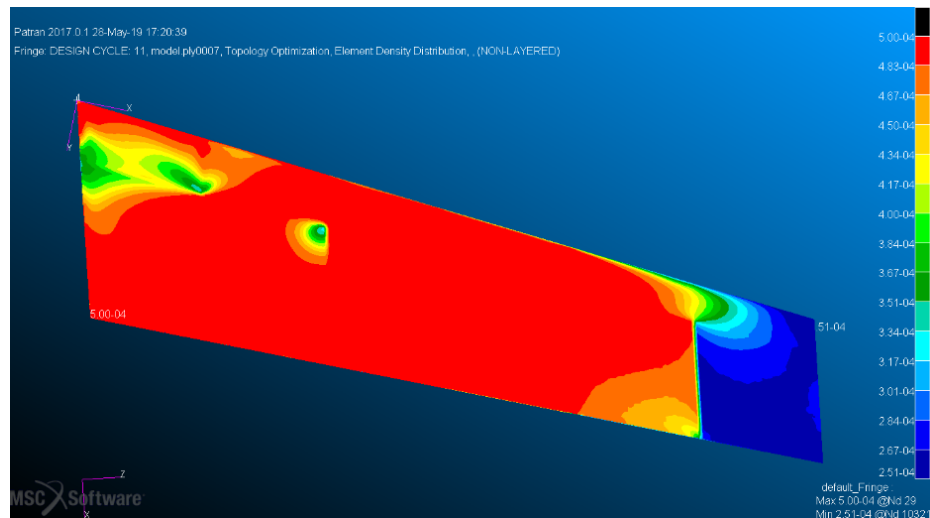


Fig. 4.26. Thickness distribution of Ply7: Lower Skin.

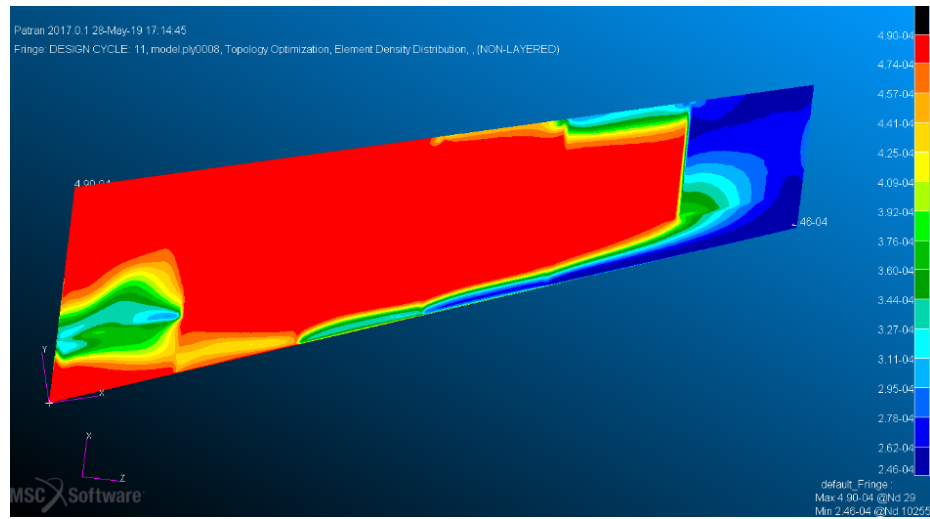


Fig. 4.27. Thickness distribution of Ply8: Upper Skin.

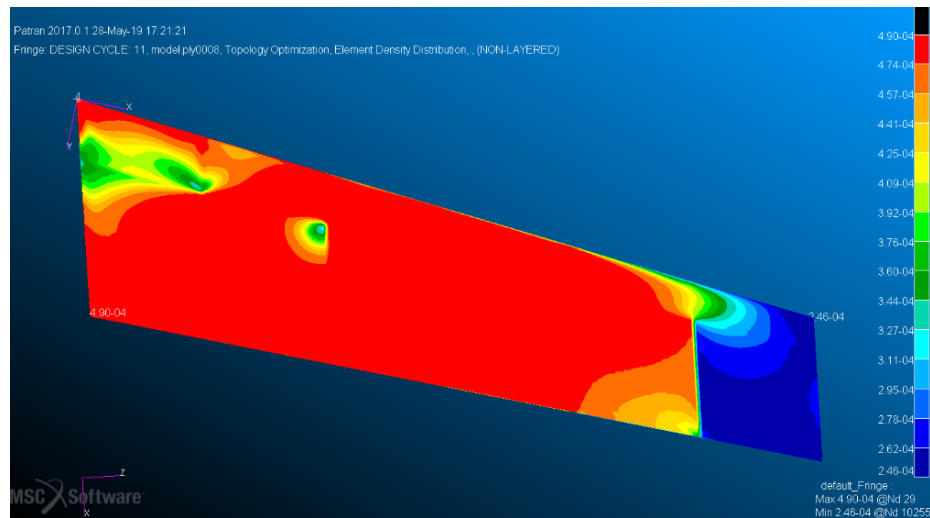


Fig. 4.28. Thickness distribution of Ply8: Lower Skin.

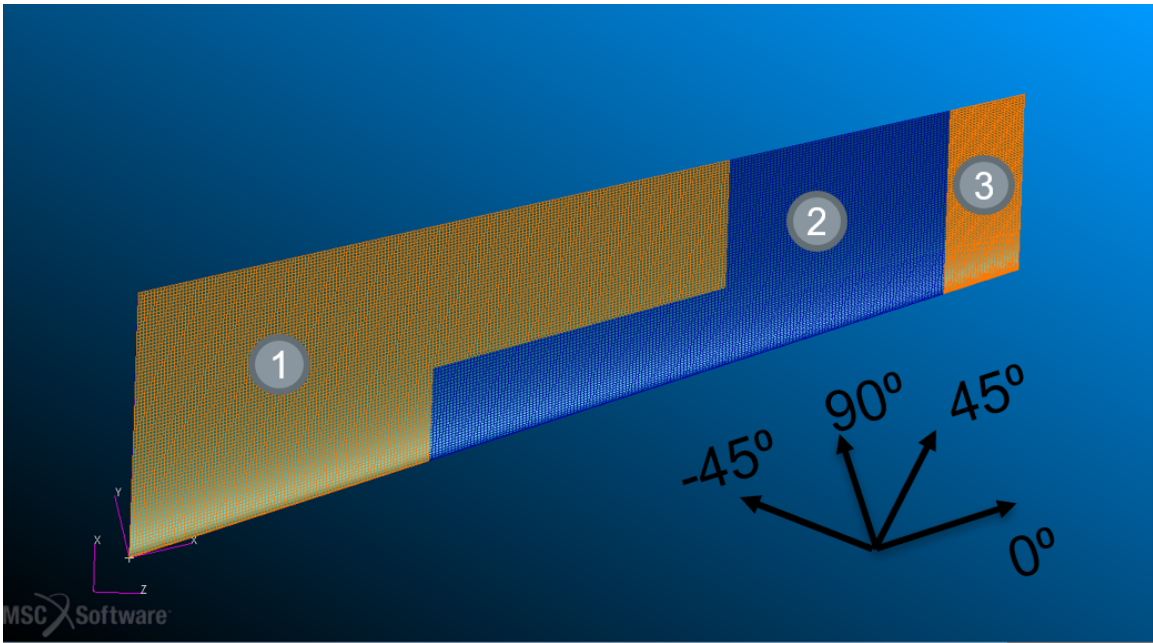


Fig. 4.29. Wing model setup for Optimization: Upper Skin.

Step 3: Size Optimization

The ply thicknesses are optimized for the applied load keeping the ply orientations constant. The model is divided into 3 areas according to the results from the topology optimization. Area 1 has a stackup of $[0^\circ/0^\circ/45^\circ/0^\circ/0^\circ/-45^\circ/90^\circ/-45^\circ]_s$. Area 2 has a stackup of $[0^\circ/0^\circ/45^\circ/0^\circ/0^\circ/-45^\circ/90^\circ]_s$. Area 3 has a stackup of $[0^\circ/0^\circ/0^\circ/0^\circ]_s$. Figure 4.29 & 4.30 shows the model setup for the optimization. Table 4.4 shows the final values for the ply orientation and thicknesses.

Once the final thickness of the super ply is obtained, the number of plies in that orientation is obtained by dividing the thickness of the super ply by the actual thickness of the ply and rounding up to the next integer.

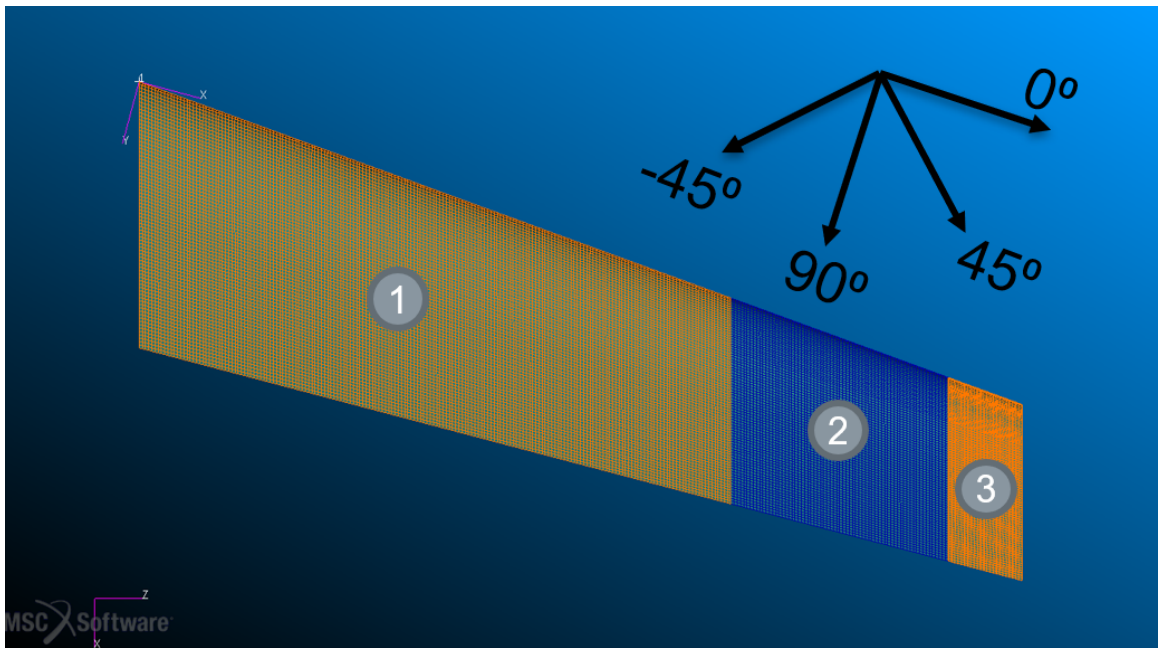


Fig. 4.30. Wing model setup for Optimization: Lower Skin.

Table 4.4.
Initial and Optimized Ply Thicknesses and Orientations

Thicknesses and Ply Orientations	Initial values		Optimized values	
Ply1	-45°	0.511 mm	-45°	0.786 mm
Ply2	90°	0.512 mm	90°	0.100 mm
Ply3	-45°	0.503 mm	-45°	0.169 mm
Ply4	0°	0.492 mm	0°	0.124 mm
Ply5	0°	0.500 mm	0°	0.123 mm
Ply6	45°	0.491 mm	45°	0.711 mm
Ply7	0°	0.501 mm	0°	0.188 mm
Ply8	0°	0.491 mm	0°	0.211 mm

5. CONCLUSION

A parametric commercial aircraft was designed in ESP. The geometry and the internal structure were designed to be regenerated by changing a few numbers. An API was created to perform optimization on a parametric wing for material failure and stability. ESP was used to create a parametric model of the wing with all components of the wing attributed and readable by the API. The wing was optimized and the geometric properties and the thicknesses of different parts of the wing were calculated. A methodology for optimization of a composite wing was proposed. The procedure was carried out on a flat plate first, and then on the wing and the ply stackup. Ply orientations and the number of plies in each orientation were calculated.

REFERENCES

REFERENCES

- [1] Engineering Sketch Pad, “ESP Beta,” <https://acdl.mit.edu/ESP/>, accessed June 2019.
- [2] R. Haimes and J. Dannenhoffer, “The engineering sketch pad: A solid-modeling, feature-based, web-enabled system for building parametric geometry,” in *21st AIAA Computational Fluid Dynamics Conference*, 2013, p. 3073.
- [3] J. Dannenhoffer, “Opencsm: An open-source constructive solid modeler for mdao,” in *51st AIAA Aerospace Sciences Meeting including the New Horizons Forum and Aerospace Exposition*, 2013, p. 701.
- [4] R. Haimes and M. Drela, “On the construction of aircraft conceptual geometry for high-fidelity analysis and design,” in *50th AIAA Aerospace sciences meeting including the new horizons forum and aerospace exposition*, 2012, p. 683.
- [5] N. D. Bhagat and E. J. Alyanak, “Computational geometry for multi-fidelity and multi-disciplinary analysis and optimization,” in *52nd Aerospace Sciences Meeting*, 2014, p. 188.
- [6] M. P. Bendsøe and N. Kikuchi, “Generating optimal topologies in structural design using a homogenization method,” *Computer methods in applied mechanics and engineering*, vol. 71, no. 2, pp. 197–224, 1988.
- [7] M. Zhou and G. I. N. Rozvany, “The coc algorithm, part ii: Topological, geometrical and generalized shape optimization,” *Computer methods in applied mechanics and engineering*, vol. 89, pp. 309–336, 1991.
- [8] G. I. N. Rozvany, M. P. Bendsøe, and U. Kirsch, “Layout optimization of structures,” *Applied Mechanics Reviews*, vol. 48, no. 2, pp. 41–119, 1995.
- [9] M. P. Bendsøe and O. Sigmund, “Topology optimization: Theory, methods and applications,” pp. 382–412, 2003.
- [10] M. Zhou, N. Pagaldipti, H. L. Thomas, and Y. K. Shyy, “An integrated approach to topology, sizing, and shape optimization,” *Structural and Multidisciplinary Optimization*, vol. 26, no. 5, pp. 308–317, 2004.
- [11] L. Krog, A. Tucker, and G. Rollema, “Application of topology, sizing and shape optimization methods to optimal design of aircraft components,” in *Proc. 3rd Altair UK HyperWorks Users Conference*, 2002.
- [12] L. Krog, A. Tucker, M. Kemp, and R. Boyd, “Topology optimisation of aircraft wing box ribs,” in *10th AIAA/ISSMO multidisciplinary analysis and optimization conference*, 2004, p. 4481.
- [13] MSC Nastran, “Design Sensitivity and Optimization User’s Guide,” <https://www.mscsoftware.com/application/design-optimization/>, accessed May 2019.